CrossMark

OSU-A9 inhibits angiogenesis in human umbilical vein endothelial cells via disrupting Akt–NF-κB and MAPK signaling pathways

Hany A. Omar [a,b], El-Shaimaa A. Arafa [b], Samir A. Salama [c], Hany H. Arab [d], Chieh-Hsi Wu [e,*], Jing-Ru Weng [f,**]

[a] Division of Medicinal Chemistry, College of Pharmacy, The Ohio State University, Columbus, OH 43210, USA
[b] Department of Pharmacology, Faculty of Pharmacy, Beni-Suef University, Beni-Suef 62514, Egypt
[c] Department of Biochemistry, Faculty of Pharmacy, Al-Azhar University, Cairo 11511, Egypt
[d] Department of Biochemistry, Faculty of Pharmacy, Cairo University, Cairo 11562, Egypt
[e] School of Pharmacy, China Medical University, Taichung 40402, Taiwan
[f] Department of Biological Science and Technology, China Medical University, Taichung 40402, Taiwan

ABSTRACT

Since the introduction of angiogenesis as a useful target for cancer therapy, few agents have been approved for clinical use due to the rapid development of resistance. This problem can be minimized by simultaneous targeting of multiple angiogenesis signaling pathways, a potential strategy in cancer management known as polypharmacology. The current study aimed at exploring the anti-angiogenic activity of OSU-A9, an indole-3-carbinol-derived pleotropic agent that targets mainly Akt–nuclear factor-kappa B (NF-κB) signaling which regulates many key players of angiogenesis such as vascular endothelial growth factor (VEGF) and matrix metalloproteinases (MMPs). Human umbilical vein endothelial cells (HUVECs) were used to study the *in vitro* anti-angiogenic effect of OSU-A9 on several key steps of angiogenesis. Results showed that OSU-A9 effectively inhibited cell proliferation and induced apoptosis and cell cycle arrest in HUVECs. Besides, OSU-A9 inhibited angiogenesis as evidenced by abrogation of migration/invasion and Matrigel tube formation in HUVECs and attenuation of the *in vivo* neovascularization in the chicken chorioallantoic membrane assay. Mechanistically, Western blot, RT-PCR and ELISA analyses showed the ability of OSU-A9 to inhibit MMP-2 production and VEGF expression induced by hypoxia or phorbol-12-myristyl-13-acetate. Furthermore, dual inhibition of Akt–NF-κB and mitogen-activated protein kinase (MAPK) signaling, the key regulators of angiogenesis, was observed. Together, the current study highlights evidences for the promising anti-angiogenic activity of OSU-A9, at least in part through the inhibition of Akt–NF-κB and MAPK signaling and their consequent inhibition of VEGF and MMP-2. These findings support OSU-A9's clinical promise as a component of anticancer therapy.

Introduction

Pathological angiogenesis plays a major role in a number of diseases including cancer, rheumatoid arthritis, atherosclerosis, and other cardiovascular diseases (Folkman, 1995; Khurana et al., 2005). Since the approval of bevacizumab, an antibody specific for vascular endothelial

growth factor (VEGF), for the treatment of metastatic colorectal carcinoma, the inhibition of angiogenesis has become a major goal of anticancer drug development (Hurwitz et al., 2004). Angiogenesis involves several key steps which include endothelial cell proliferation, migration, invasion and tube formation (Nacev and Liu, 2011). Effective antiangiogenic agents should target one or more of these processes (Omar et al., 2012).

VEGF, the key angiogenic cytokine, plays a key role in angiogenesis and neovascularization and stimulates the proliferation, migration as well as tube formation of plated endothelial cells (Byrne et al., 2005). VEGF production is up-regulated in cancer cells by oncogene expression, growth factors and hypoxia (Carmeliet, 2005). The production of VEGF by cancer cells is essential for the 'angiogenic switch', where neovascularization is formed within and around the tumor promoting exponential growth (Wang et al., 2012). However, the newly formed blood vessels under the influence of VEGF are irregularly shaped, convoluted, unorganized and leaky that cause hypoxia and further VEGF production. Thus, the central role of VEGF in tumor angiogenesis makes it an optimal target for anticancer therapy.

Equally important, the matrix metalloproteinase (MMP) family is another key player in the angiogenesis process (Artacho-Cordon et al., 2012). MMPs are frequently overexpressed in malignant tumors and are implicated in the processes of tumor growth, invasion, and metastasis (Coussens et al., 2002; Roy et al., 2009). Among the structurally related human MMPs, the expression of gelatinases such as MMP-2 and MMP-9 increases in malignant cancers compared to benign cancers (Klein et al., 2004; Roomi et al., 2010). The association of MMPs with aggressive malignant phenotype and poor prognosis in cancer highlights the need for the development of MMP inhibitors (Szinwong et al., 2013).

Although few anti-angiogenic agents are currently available in the clinic, their efficacy is limited by the up-regulation of alternative and compensatory signaling pathways during the course of treatment (Abdollahi and Folkman, 2010; Bergers and Hanahan, 2008). One of the most successful strategies to minimize resistance in cancer therapy is the employment of polypharmacology to simultaneously modulate more than one target involved in a network of signaling (Reddy and Zhang, 2013). A well-recognized example of polypharmacology is sorafenib, an oral multikinase inhibitor that has been approved for the treatment of patients with advanced renal cell carcinoma and unresectable hepatocellular carcinoma (Wilhelm et al., 2008).

The unique ability of OSU-A9 to selectively induce apoptosis in various types of cancer, including prostate, breast, liver, and oral cancer with high safety margins supports its clinical development into a cancer therapeutic agent (Omar et al., 2009; Weng et al., 2007, 2009, 2010). Given that OSU-A9 has been reported to target Akt–NF-κB signaling that mediates the action of VEGF and MMPs, the key players in angiogenesis process (Cheung et al., 2011; Morais et al., 2009; Shiojima and Walsh, 2002), we aimed to investigate its potential anti-angiogenic activity that may highlight the usefulness of OSU-A9 in cancer therapy. The current work, describes for the first time, the in vitro and in vivo anti-angiogenic efficacy of OSU-A9 along with its dual inhibition of Akt–NF-κB and MAPK signaling.

Material and methods

Material. OSU-A9 [1-(4-chloro-3-nitrobenzenesulfonyl)-1*H*-indol-3-yl]-methanol was synthesized as described before (Fig. 1A) (Weng et al., 2007). The identity and purity (≥99%) of OSU-A9 were verified by proton nuclear magnetic resonance, high-resolution mass spectrometry, and elemental analysis. OSU-A9 was dissolved in dimethyl sulfoxide (DMSO) and diluted in culture medium. Endothelial Cell Growth Medium-2 (EGM-2) was purchased from Lonza (Walkersville, MD) and fetal bovine serum (FBS) from Invitrogen (Carlsbad, CA). Matrigel and 24-well modified Boyden chambers (8 μm pore size) were obtained from BD Biosciences (Bedford, MA) and Corning Costar (Cambridge, MA), respectively. Antibodies against the following biomarkers were obtained from the indicated commercial sources: procaspase-8, procaspase-3, poly (ADP-ribose) polymerase (PARP), proliferating cell nuclear antigen (PCNA), p-^{473}Ser Akt, p-^{308}Thr Akt, Akt, MMP-2, MMP-9, IKKα and p-^{108}Ser IKKα and p-^{217}Ser/^{221}Ser mitogen-activated protein kinase (MEK) from Cell Signaling Technology (Beverly, MA); p-^{180}Thr/^{182}Tyr p38, p38, Bcl-2, MEK, NF-κB, mammalian target of rapamycin (mTOR), p-^{2448}Ser mTOR, ERK, jun N-terminal kinase (JNK), p-$^{183/185}$Thr/Tyr JNK, and p-$^{202/204}$Thr/Tyr ERK from Millipore (Bedford, MA); and β-actin was obtained from Sigma-Aldrich (St. Louis, MO). Other chemicals and reagents were obtained from Sigma-Aldrich unless otherwise mentioned.

Cell culture and hypoxic conditions. Human umbilical vascular endothelial cells (HUVECs, ScienCell Research Laboratories, Carlsbad, CA) were grown in EGM-2 supplemented with 10% FBS. Cells were maintained at 37°C in a humidified incubator containing 5% CO_2. For hypoxic conditions, cells were incubated at 5% CO_2 with 1% O_2 balanced with N_2 in an anaerobic chamber (Forma Scientific). The passage number of all the used cells was between 3 and 5.

Cell cycle analysis. Treated HUVECs were harvested and washed with cold $1 \times$ PBS and then fixed with 70% ice-cold ethanol overnight. After centrifugation at $1200 \times g$ at 4 °C for 5 min, the ethanol was removed and the pellets were resuspended in 500 μL of DNA staining buffer (4 μg/mL of propidium iodide, 1% Triton X-100, and 0.1 mg/mL of RNase A) and incubated for 30 min at room temperature in the dark. Samples were subjected to flow cytometry using a FACSCanto flow cytometer (BD Biosciences, San Jose, CA), and the cell cycle profile was analyzed using the Modfit LT Program (Verify Software House, Topsham, HE).

Cell viability analysis. Cell viability was assessed using the 3-(4,5-dimethylthiazol-2-yl)-2,5-diphenyltetrazolium bromide (MTT) assay as described before (Bai et al., 2011). In brief, HUVECs were seeded at 1×10^4 cells/well in 96-well flat-bottomed plates in EGM-2. After 24 h, cells were treated with different concentrations of OSU-A9 in the presence and absence of 50 μM Pan Caspase Inhibitor Z-VAD-FMK (R&D Minneapolis, MN) in a total volume of 100 μL of 10% FBS-containing culture medium. At the end of the treatment, the media were removed, replaced by 200 μL fresh EGM-2 containing 0.5 mg/mL of MTT and cells were incubated in the CO_2 incubator at 37 °C for 2 h. Supernatants were removed by aspiration, and the reduced MTT was dissolved in 200 μL/well DMSO. Absorbance at 570 nm was determined using a plate reader. The results were calculated by subtracting blank readings, in which cells were absent, from sample readings. The cell viability was expressed as a percentage of the vehicle-treated control group. For cell count analysis, HUVECs were seeded overnight in 6-well plates at 1.2×10^5 cells/well and were treated at the indicated concentrations of OSU-A9 or vehicle for 24 h. At the end of the treatment, cells were washed three times with PBS and trypsinized. Cell numbers were calculated using Coulter Z1 cell counter (Beckman Coulter).

Western blotting. Lysates of HUVECs treated with OSU-A9 at the indicated concentrations for 24 h were prepared for immunoblotting of procaspase-8, procaspase-3, PARP, p-^{473}Ser Akt, p-^{308}Thr Akt, Akt, MMP-2, MMP-9, IKKα and p-^{108}Ser IKKα and p-^{217}Ser/^{221}Ser MEK, p-^{180}Thr/^{182}Tyr p38, p38, Bcl-2, MEK, NF-κB, mTOR, p-^{2448}Ser mTOR, ERK, JNK, p-$^{183/185}$Thr/Tyr JNK, p-$^{202/204}$Thr/Tyr ERK, PCNA and β-actin. Western blot analysis was performed as previously reported (Kulp et al., 2006).

Preparation of nuclear extracts. Cells were treated with different concentrations of OSU-A9 for 24 h. Nuclear extracts were prepared using NEPER Nuclear and Cytoplasmic Extraction Reagents Kit (PIERCE®, Rockford, IL) according to the manufacturer's instructions. Nuclear extracts were then analyzed for NF-κB levels by western blotting as described above.

DAPI staining assay. HUVECs at the density of 4×10^4 cells/well in 24-well plates were incubated with the indicated concentrations of OSU-A9 or vehicle (DMSO) for 24 h in EGM-2 medium containing 10% FBS. Harvested HUVECs were stained by 4′,6-diamidino-2-phenylindole (DAPI) then examined and photographed by using a fluorescence microscope.

Matrigel tube formation assay. *In vitro* anti-angiogenic activity of OSU-A9 was conducted using Matrigel tube formation assay as described before (Chabut et al., 2003). In summary, Matrigel (10 mg/mL, 100 μL) was incubated for 30–45 min at 37 °C for polymerization to take place. HUVECs suspended in 300 μL EGM-2 supplemented with 10% FBS at a density of 4×10^4 cells/mL were added to Matrigel-coated plates. Different concentrations of OSU-A9 or vehicle were added
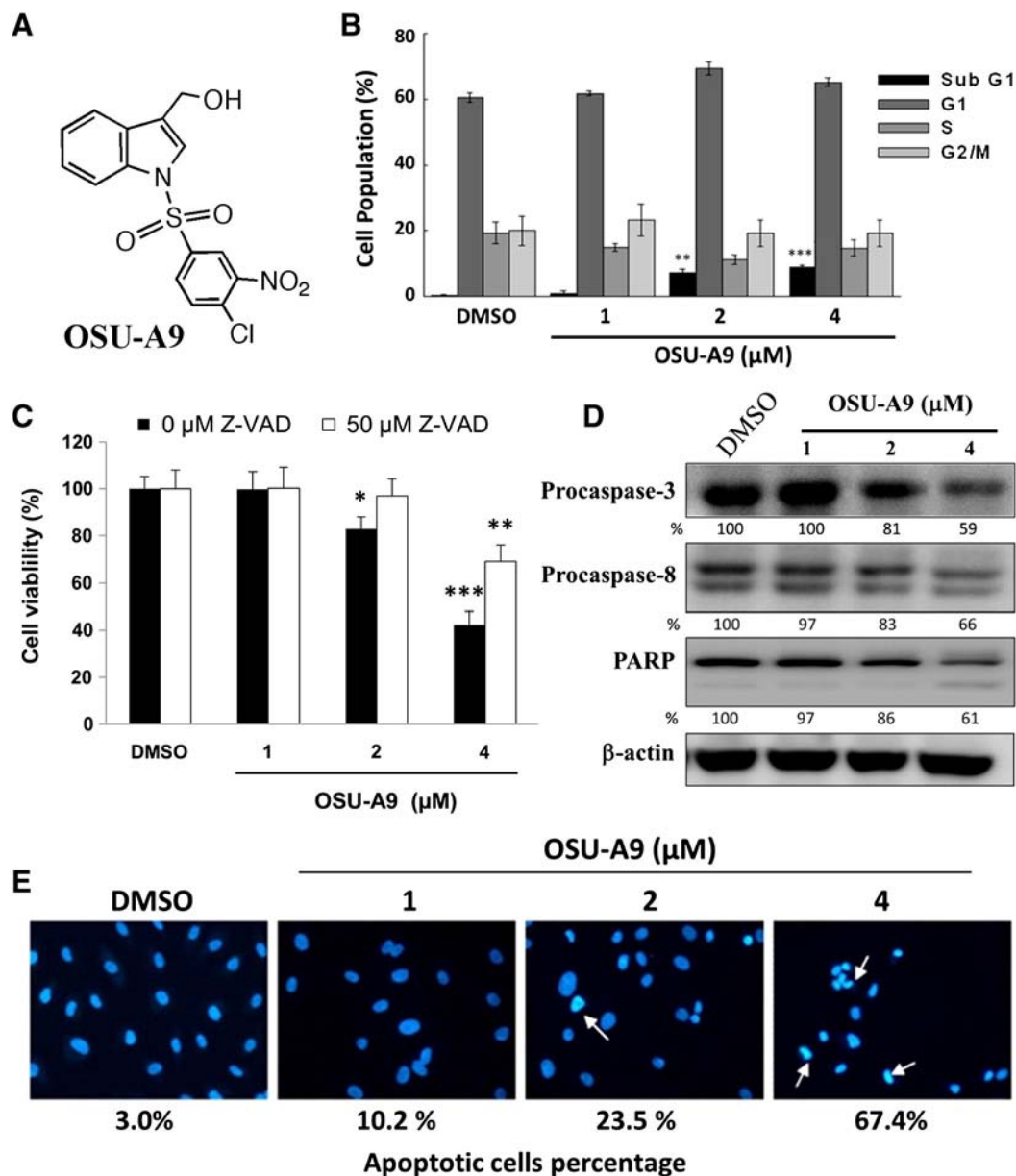
Fig. 1. The anti-proliferative activity of OSU-A9 on HUVECs. (A) Structure of OSU-A9. (B) Cell cycle analysis by flow cytometry in HUVECs after treatment with DMSO vehicle or the indicated concentrations of OSU-A9 for 24 h. Histogram showing dose-dependent effects of OSU-A9 on cell cycle distribution. Columns, mean; bars, S.D. (n = 5). **$P < 0.01$, ***$P < 0.001$ as compared to vehicle-treated cells. (C) Dose-dependent effect of OSU-A9 on the cell viability of HUVECs after 24 h treatment in presence and absence of 50 μM Z-VAD-FMK as measured by MTT. Columns, mean; bars, S.D. (n = 6). *$P < 0.05$, **$P < 0.01$, ***$P < 0.001$ as compared to vehicle (DMSO)-treated cells. (D) Western blot analysis of cell lysates from HUVEC after treatment with OSU-A9 or DMSO vehicle for 24 h. (E) DAPI staining of HUVECs showing pyknotic nuclei (arrows) as an indicator of apoptosis after 24 h of the indicated treatments.

to the cell suspension and incubated at 37 °C for 12 h. Tube formation was observed with an inverted phase contrast microscope (Nikon Corporation, Tokyo, Japan).

Chorioallantoic membrane assay. For *in vivo* anti-angiogenic activity, chorioallantoic membrane (CAM) was performed as previously described (Liekens et al., 2006). Fertilized chicken eggs were incubated at 37 °C for 3 days in a humidified incubator. Hypodermic needles were used to remove 4 mL of egg albumin to allow the detachment of the shell from the developing CAM. An opening in the eggshell was made to expose the CAM and the opening was then covered with cellophane tape and re-incubated. OSU-A9 or vehicle loaded on sterile plastic discs (8 mm) and allowed to dry under sterile conditions was placed on CAM on the 9th day. Retinoic acid (RA) was used as a positive control anti-angiogenic compound. The eggs were further incubated for two more days then the plastic discs

were removed and the membranes were fixed by 7% buffered formalin. After fixation, the membranes were observed under a microscope and blood vessels were counted.

Migration assays. Modified Boyden chambers (8 μm; Corning Costar, Cambridge, MA) were used as mentioned before (Omar et al., 2009). Briefly, HUVECs (7×10^5/well) in 0.5 mL of serum-free medium containing the indicated concentration of OSU-A9 or the vehicle were seeded into the upper chamber insert, and incubated at 37 °C for 60 min. The inserts were then switched to a new well containing the same concentration of OSU-A9 or vehicle in 10% FBS-supplemented medium, and incubated for 8 h. Cells on the upper surface of each filter were scraped off thoroughly with cotton swabs, while cells on the underside of the filter were fixed in 90% methanol and stained with 5% Giemsa (Merck, Darmstadt, Germany). For each chamber, the number of migrated cells was counted in ten randomly chosen 200× fields.

Invasion assays. HUVECs (7×10^5/well) were suspended in 0.5 mL of serum-free medium containing the indicated concentration of OSU-A9 or vehicle. The cell suspensions were seeded onto Matrigel-coated or uncoated membranes of the upper chambers of modified Boyden chambers (8 μm; Corning Costar, Cambridge, MA) and incubated at 37 °C. The lower chambers contained the same amount of OSU-A9 or vehicle in 10% FBS-containing medium. After 24 h, all the cells remaining on the upper surface of the membranes were removed with cotton swabs. Cells on the lower surface of the membrane were fixed in 90% methanol and stained with 0.1% crystal violet for 10 min. The cells on each membrane were counted in ten 200× fields. Tumor cell invasion was expressed as the number of cells that had passed through the Matrigel-coated membranes.

Measurement of VEGF. Enzyme-linked immunosorbent assay was employed to measure VEGF concentration. Briefly, cells were treated with OSU-A9 or vehicle and incubated for 24 h in the hypoxia chamber. The VEGF concentration in the media was determined using a VEGF Immunoassay kit (R&D Systems, Minneapolis, MN) according to the manufacturer's instructions. The results were expressed as fold change in the concentration of VEGF relative to that of cells under non-hypoxic condition (normoxia).

Reverse transcriptase-polymerase chain reaction (RT-PCR) analysis.
RT-PCR analysis was performed as mentioned before with few modifications (Arafa el et al., 2011). In summary, HUVECs were treated with OSU-A9 for 24 h in the presence and absence of 50 nM phorbol-12-myristyl-13-acetate (PMA). Total RNA was then extracted using the TRIzol® reagent (Invitrogen, Carlsbad, CA). RT-PCR was run using a one-step RT-PCR kit and β-actin was used as an internal control to normalize input cDNA. The used forward primers for VEGF-A and β-actin were 5′-GGGCAGAATCATCACGAAGT-3′ and 5′-GTGGGGCGCCCCAGG CACCA-3′, respectively. The reverse primers for VEGF and β-actin were 5′-ATCTGCATGGTGATGTTGGA-3′ and 5′-CTCCTTAATGTCACGCAC GATT-3′, respectively. The amplified PCR products were separated on 2% agarose gel, stained with ethidium bromide and viewed under ultraviolet light. The integrated absorbance values of the VEGF and β-actin bands were analyzed using the Bio-Rad image system semi-quantitative analysis.

Gelatin zymography. Briefly, conditioned media from HUVECs treated with different concentrations of OSU-A9 in the absence of serum for 24 h were collected. Samples were mixed with loading buffer and then electrophoresed on SDS-polyacrylamide gels containing 0.1% gelatin. After removing SDS with 2.5% Triton-X100 solution, the gel was incubated with zymogen developing buffer and then stained with Coomassie Blue R-250. The enzyme-digested regions, observed as clear bands in destained gel against a blue background, indicated the presence of MMP-2 and MMP-9. The visualized bands were quantitated after normalization to 10% FBS DMSO-vehicle using the digital imaging analysis system.

Statistical analysis. Differences among group means were analyzed for statistical significance using one-way ANOVA followed by the Neuman–Keuls test for multiple comparisons. Differences were considered significant at $P < 0.05$. Statistical analysis was performed using SPSS for Windows (SPSS, Inc., Chicago, IL).

Results

OSU-A9 inhibits HUVEC growth by the induction of apoptosis

Local proliferation of endothelial cells is the first step in the angiogenic process. The anti-proliferative effect of OSU-A9 (Structure, Fig. 1A) on HUVECs was assessed by both cell cycle distribution analysis and MTT assay. Flow cytometric analysis of OSU-A9-treated HUVECs revealed the accumulation of sub-G1 cells at 2 and 4 μM, as compared to vehicle-treated control (Fig. 1B). MTT results showed that OSU-A9 inhibited the cell viability of HUVECs after 24 h treatment in a dose-dependent manner. The half maximal inhibitory concentration (IC_{50}) of OSU-A9 was 3.2 μM after 24 h treatment in 10% FBS-supplemented EGM-2 medium (Fig. 1C). The pan caspase inhibitor, Z-VAD-FMK, was used to confirm that the OSU-A9-induced inhibition of cell viability was mediated through the induction of apoptosis. Z-VAD-FMK was able to partially rescue HUVECs from the action of OSU-A9 which indicates that the inhibition of HUVEC viability by OSU-A9 is mediated, at least in part, via the activation of caspases. Western blot analysis of OSU-A9-treated HUVECs for 24 h revealed the hallmarks of apoptosis such as the increase in PARP cleavage and the decrease in procaspases -3 and -8. (Fig. 1D, and Suppl. Table 1). The induction of apoptosis was further confirmed by DAPI nuclear staining. The nuclear morphology revealed chromatin condensation, which was visualized as intense bluish-white fluorescence in pyknotic nuclei (Fig. 1E and Suppl. Table 2). Together, these data indicate that the anti-proliferative effects of OSU-A9 in HUVECs are attributable, at least in part, to the induction of apoptosis.

OSU-A9 exhibits anti-angiogenic activity both in vitro and in vivo

Angiogenesis plays a major role in the process of metastasis and tumor progression. *In vitro* anti-angiogenic assays were carried out in HUVECs to test the specific effect of OSU-A9 on several key players of the angiogenic process such as tube formation. The final event during angiogenesis is the alignment of endothelial cells into a network of tubes. Since HUVECs arrange themselves in a three-dimensional tube-like network when plated on a matrix, Matrigel tube formation assay was used to test the anti-angiogenic activity of OSU-A9 *in vitro*. OSU-A9 tapered the HUVEC tube formation ability in Matrigel in a dose-dependent manner (Fig. 2A). As shown in the representative images of Matrigel tube formation assay, the anti-angiogenic effect of OSU-A9 was observed even at 1 μM concentration. CAM assay was employed to test the ability of OSU-A9 to inhibit neovascularization in vivo (Fig. 2B). Images of illustrative CAMs and the quantified data of vascular density after treatment showed the ability of OSU-A9 to inhibit the angiogenesis in CAMs which was comparable to that of RA, a well-known anti-angiogenic agent.

OSU-A9 inhibits cell migration/invasion of HUVECs in vitro

The ability of OSU-A9 to antagonize endothelial cell migration/invasion was analyzed by modified Boyden's chamber assay. Only endothelial cells with high migratory ability can pass through the Boyden's chamber membrane of 8 μm pore. OSU-A9 effectively diminished the migratory ability of endothelial cells through the porous inserts (Fig. 2C). In addition, OSU-A9 inhibited the ability of HUVECs to invade Matrigel-coated membranes (Fig. 2D) in a dose-dependent manner. OSU-A9 was highly effective, even at 1 μM concentration indicating a more potent effect on cell migration/invasion than growth inhibition as measured by MTT (IC_{50}, 3.2 μM). This discrepancy might be attributable to differences in the used medium (i.e., serum-free EGM-2 for migration/invasion assays versus 10% FBS-supplemented EGM-2 for MTT assays). Similar effect of OSU-A9 was observed in hepatocellular carcinoma where the serum-free medium gave rise to high potency due to the lack of protein binding of drug molecules and growth factors (Omar et al., 2009).

OSU-A9 inhibits VEGF and MMP-2 expression in HUVECs

Since VEGF and MMPs play a central role in angiogenesis and neovascularization, we assessed the ability of OSU-A9 to suppress the expression of VEGF and MMPs in HUVECs. VEGF expression was induced either by hypoxia or PMA. OSU-A9 significantly inhibited, in a
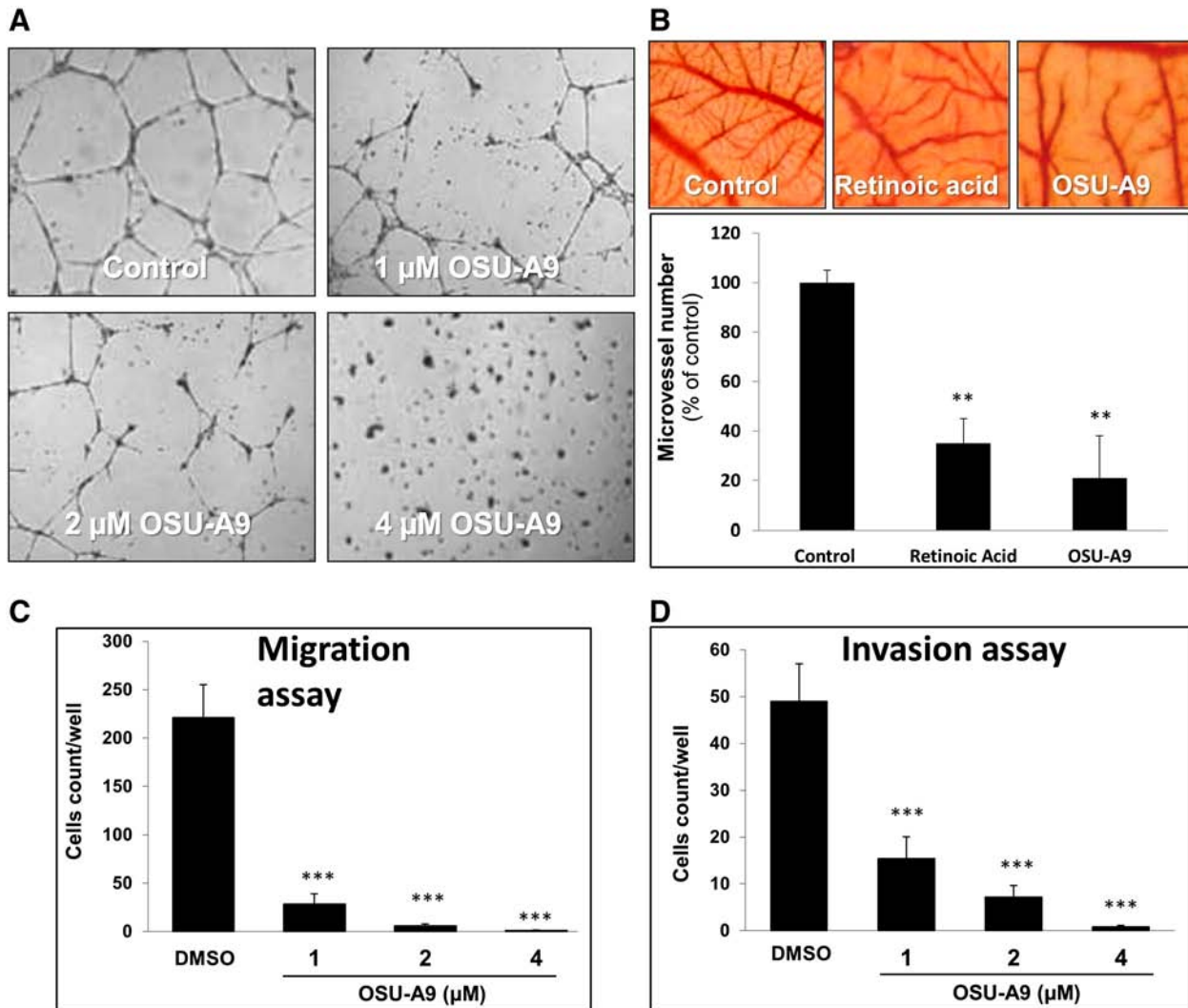
Fig. 2. *In vitro* and in vivo inhibitory activity of OSU-A9 on angiogenesis, migration and invasion. (A) Effect of OSU-A9 on the tube-forming ability of HUVECs in Matrigel. (B) Effect of OSU-A9 on neovascularization in the CAM assay. CAMs of fertile eggs were treated with OSU-A9 (2 μg/egg), RA (2 μg/egg) or vehicle for 48 h. *Upper panel*, representative images of CAMs after the indicated treatments. *Lower panel*, vascular density expressed as percentage of blood vessel branches relative to vehicle-treated CAMs. Columns, mean; bars, S.D. (n = 6). **$P < 0.01$ as compared to DMSO (vehicle) treatments. (C) Dose-dependent effects of OSU-A9 on HUVEC migration. Columns, mean; bars, S.D. (n = 10). ***$P < 0.001$ as compared to control DMSO treatments. (D) OSU-A9 inhibitory activity on HUVEC invasion. Columns, mean; bars, S.D. (n = 10). ***$P < 0.001$ as compared to DMSO treatments.

dose-dependent manner, hypoxia-induced expression of VEGF which was measured in the medium by ELISA (Fig. 3A). Furthermore, the RT-PCR results showed that PMA-induced expression of VEGF in HUVECs was inhibited by varying concentrations of OSU-A9 (Fig. 3B). To determine the effect of OSU-A9 on endothelial cell production of MMP-2 and MMP-9, HUVECs were treated with various concentrations of OSU-A9 for 24 h, and the presence of the secreted forms of MMP-2 and MMP-9 in the conditioned medium was analyzed using gelatin zymography. As shown in Fig. 3C (upper panel), treatment with OSU-A9 at 2 or 4 μM reduced the proteolytic activity of MMP-2 by 37% and 69%, respectively, while that of MMP-9 was not noticeably affected. This OSU-A9-induced reduction in MMP-2 proteolytic activity was confirmed by western blot analysis which demonstrated the ability of OSU-A9 to reduce the expression of MMP-2 in HUVECs (Fig. 3C, lower panel). To exclude the possibility that the reduction of VEGF and MMP-2 could be secondary to OSU-A9-induced cytotoxicity, cell number analysis was performed. Results showed that a significant reduction in cell number caused by OSU-A9 in HUVECs could be observed only at concentrations above the IC$_{50}$, at 4 μM (Fig. 3D). On the other hand, a significant inhibition of VEGF and MMP-2 occurs at relatively lower

concentrations, 1 and 2 μM, which rule out the possibility that VEGF and MMP-2 inhibition is a direct result of OSU-A9-induced cytotoxicity.

OSU-A9 targets the Akt, NF-κB and MAPK signaling pathways in HUVECs

OSU-A9 is a pleotropic agent that effectively targets multiple signaling pathways (Weng et al., 2007). To gain an insight into the anti-angiogenic mechanisms of OSU-A9 in HUVECs, its ability to target several signaling pathways involved in angiogenesis was examined. The Akt and NF-κB signaling pathways have been reported to regulate multiple critical steps in angiogenesis in HUVECs (Morais et al., 2009; Singh et al., 2005; Tammali et al., 2011). Our previous work demonstrated the ability of OSU-A9 to target Akt/NF-κB signaling in hepatocellular carcinoma (Omar et al., 2009), breast cancer (Weng et al., 2009) and oral cancer (Weng et al., 2010) with an IC$_{50}$ values ranging from 1.2 to 3.2 μM, so we examined the effect of OSU-A9 on these pathways in HUVECs. Western blot analysis showed the ability of OSU-A9 to inhibit Akt/NF-κB signaling in a dose-dependent manner (Fig. 4A, left panel and Suppl. Table 3). OSU-A9 reduced the levels of p-[308]Thr-Akt, p-[473]Ser-Akt as well as the Akt-dependent survival factor, p-mTOR.
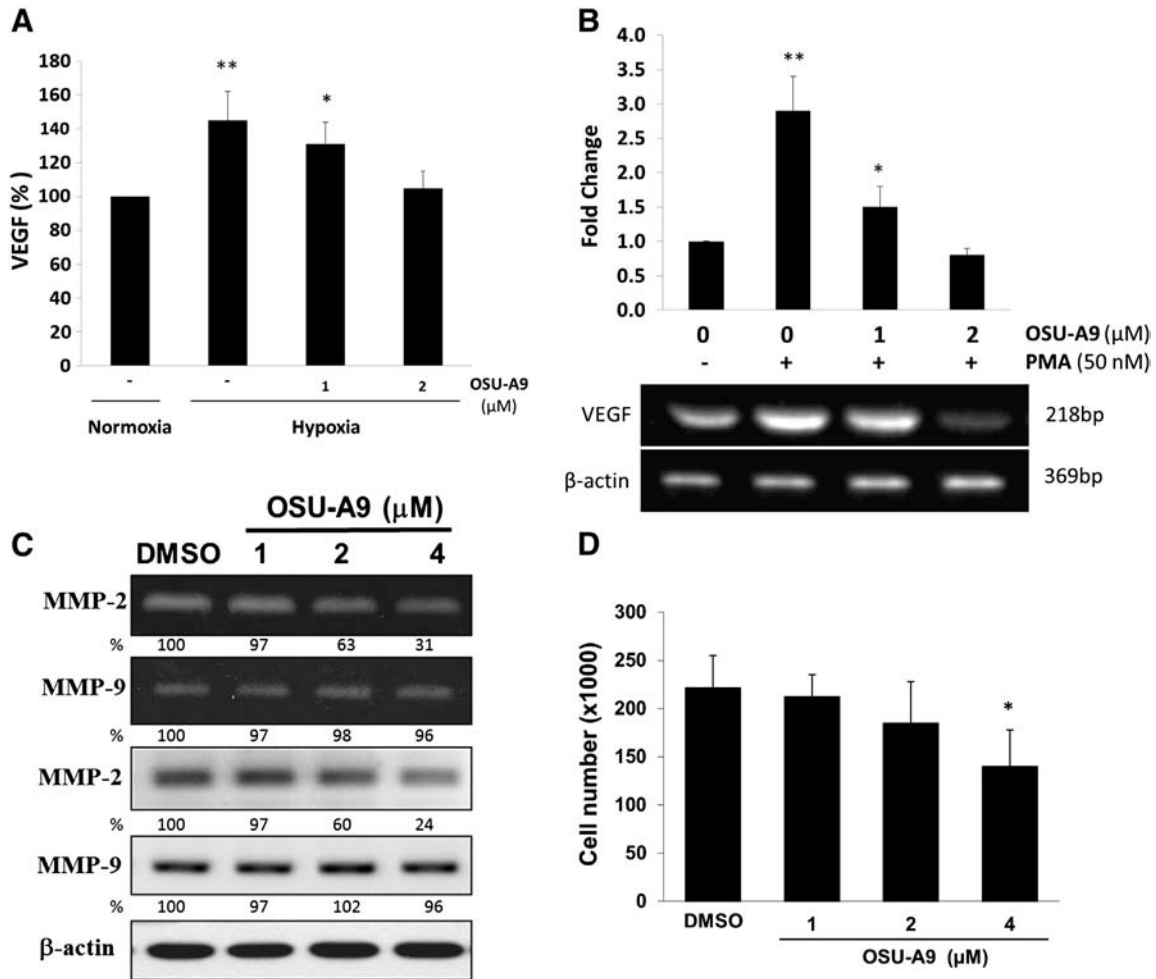
Fig. 3. OSU-A9 inhibited vascular VEGF and MMP-2 expression in HUVECs. (A) OSU-A9 inhibits hypoxia-induced VEGF production in HUVECs. Columns, mean; bars, S.D. (n = 6). *P < 0.05, **P < 0.01 as compared to cells under normoxia. (B) RT-PCR analysis showing the ability of OSU-A9 to inhibit PMA-induced VEGF expression in HUVECs. *Upper panel*, graph depicting fold changes of the VEGF cDNA relative to vehicle-treated cells and normalized with β-actin expression level. Columns, mean; bars, S.D. (n = 6). *P < 0.05, **P < 0.01 as compared to vehicle (DMSO)-treated cells under normoxia. *Lower panel*, the PCR products resolved on 2% agarose gel. (C) Effects of OSU-A9 on the activity and expression of MMP-2 and MMP-9 after 24 h treatment. *Upper panel*, levels of MMP-2 and MMP-9 secreted into the cultured medium were determined by gelatin zymography. *Lower panel*, western blot analysis of the expression of MMP-2 and MMP-9 in treated HUVECs. (D) Effects of OSU-A9 on the cell number of HUVECs after 24 h treatment. Columns, mean; bars, S.D. (n = 6). *P < 0.05 as compared to vehicle-treated cells.

The data also indicated that OSU-A9 inhibited NF-κB signaling in HUVECs through two distinct mechanisms. First, OSU-A9 inhibited the phosphorylation of IKKα which would prevent the inactivation of the NF-κB inhibitor, IκB, by ubiquitination. Second, the NF-κB-dependent survival factors Bcl-2 and Bcl-xL were also reduced in OSU-A9-treated cells (Fig. 4A). Finally, OSU-A9 reduced the level of the RelA/p65 subunit of NF-κB in the nucleus of HUVEC (Fig. 4B).

The inhibition of Akt/NF-κB signaling was accompanied by parallel decreases in the phosphorylation levels of many members of the MAPK signaling pathway such as MEK, MAP kinases ERKs, p38, and JNK (Fig. 4A, right panel and Suppl. Table 3). MAPKs are implicated in many aspects of tumorigenesis including angiogenesis (Tang et al., 2010; Tate et al., 2013) and the inhibition of MAPK causes inhibition of VEGF-induced cell proliferation and angiogenesis in HUVECs (Wu et al., 2000, 2006).

Discussion

Angiogenesis involves many key steps which include endothelial cell proliferation, migration, invasion and tube formation (Nacev and Liu, 2011). Here, we report the antiangiogenic activity of OSU-A9, a pleotropic agent that has been shown to inhibit cell proliferation in various types of cancer, including prostate, breast, liver, and oral cancer, through the inactivation of Akt–NF-κB signaling (Omar et al., 2009; Weng et al., 2007, 2009, 2010).

Our data showed that OSU-A9 inhibited the proliferation of HUVECs in a dose-dependent manner. Mechanistically, the anti-proliferative activity of OSU-A9 in HUVECs was mediated, at least in part, through the inhibition of Akt, NF-κB and MAPK signaling pathways and the induction of apoptosis. Moreover, OSU-A9 inhibited the tube forming ability of HUVECs *in vitro* and *in vivo* neovascularization in the chicken CAM at concentrations below 4 μM. These methods, by which endothelial cells form 3D capillary like structure, are considered as the most widely used *in vitro* models for evaluating angiogenesis.

Since VEGF plays a key role in promoting angiogenesis and this action is mediated through Akt–NF-κB signaling (Kitamura et al., 2008; Morais et al., 2009), we investigated the effect of OSU-A9 on VEGF expression induced by hypoxia or PMA. Results showed the ability of OSU-A9 to counteract both hypoxia and PMA-induced VEGF gene expression in HUVECs. The extent of inhibition of VEGF expression by OSU-A9, prompted us to confirm the anti-angiogenic activity by studying its effect on other key steps involved in angiogenesis process such as
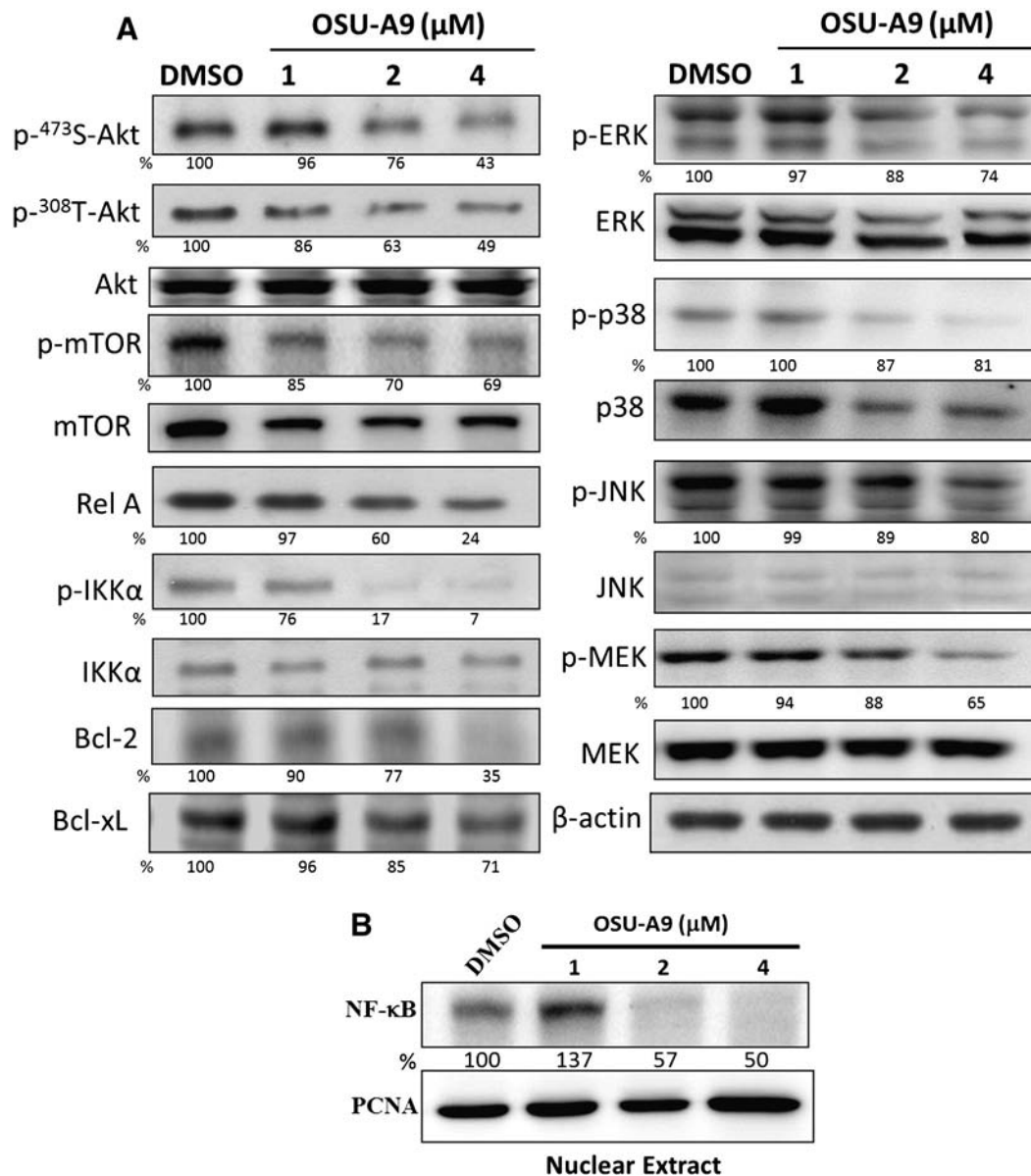
Fig. 4. Effect of OSU-A9 on angiogenesis-related signaling pathways in HUVECs. (A) Western blot analysis of the phosphorylation and/or expression level of Akt, mTOR, RelA, IKKα, Bcl-2, Bcl-xL, ERK, p38, JNK and MEK. The values denote percentage of changes as determined by the relative intensity of protein bands of treated samples to that of the corresponding vehicle-treated control after normalization to the internal reference, β-actin. Cells were treated with the indicated concentrations of OSU-A9 for 24 h. Each value represents the average of three independent experiments. (B) Western blot analysis of the nuclear expression of NF-κB. Nuclear extracts were isolated from HUVECs treated with OSU-A9 for 24 h. PCNA was used as a nucleus-specific loading control. Each value represents the average of three independent experiments.

endothelial cell migration/invasion. OSU-A9 effectively diminished endothelial cell migration/invasion analyzed by modified Boyden's chamber assay.

MMPs, a group of Zn-dependent endopeptidases, contribute to cancer cell invasion and metastasis, as well as tumor angiogenesis (Waas et al., 2002; Wang et al., 2003). It has been reported that the migration and invasion of breast cancer cells were inhibited by indole-3-carbinol, the parent drug of OSU-A9 (Hung and Chang, 2009). Our gelatin zymography results and western blot analysis revealed that OSU-A9 reduced MMP-2 protein expression and secretion in HUVECs suggesting that MMP-2 is one of the antiangiogenic targets of OSU-A9 in endothelial cells. Evidence has indicated that MMP-2 expression is regulated by MAPK members and the Akt pathway (Schram et al., 2010; Yue et al., 2011). Therefore, we examined the effect of OSU-A9 on the expression and/or phosphorylation status of the components of the MAPK and Akt signaling pathways in HUVECs. Results showed that OSU-A9 significantly reduced JNK, ERK, p38, Akt, and mTOR

phosphorylation, suggesting the inhibition of MAPK and Akt signaling in OSU-A9-treated endothelial cells. Furthermore, OSU-A9 inhibited NF-κB, a pro-inflammatory transcription factor associated with angiogenesis (Dell'Eva et al., 2007), through the suppression of IKKα phosphorylation and p65 nuclear translocation.

In summary, our former studies about OSU-A9 proved its ability to selectively target cancer cells with high safety margins via the inhibition of Akt–NF-κB signaling network. The current work demonstrated the antiangiogenic activity of OSU-A9 in the *in vitro* HUVEC model and the *in vivo* CAM assay via disrupting Akt–NF-κB and MAPK signaling with consequent inhibitory effects on VEGF and MMP-2 expression as well as endothelial cell proliferation, migration/invasion and *in vitro* tube formation (Fig. 5). Together, these findings reveal a new therapeutic application for OSU-A9 as an anti-angiogenic agent and underscore the translational value of OSU-A9 as a new therapeutic candidate for cancer. It warrants attention that OSU-A9 lacks comprehensive pharmacokinetic studies that are required as a critical preceding step to clinical trials.
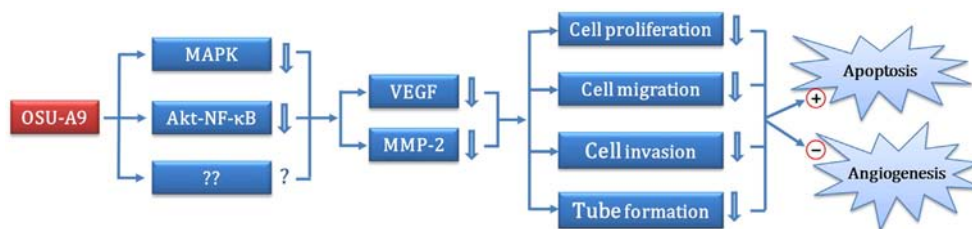
Fig. 5. Diagram depicting the potential anti-angiogenic mechanisms of OSU-A9 in HUVECs.

Consequently, further preclinical safety studies are thus required to determine the therapeutic index of OSU-A9 before its use in humans.

Conflict of interest

None of the listed authors has any financial or other interests that could be of conflict.

Acknowledgments

Appendix A. Supplementary data

Supplementary data to this article can be found online at http://dx.doi.org/10.1016/j.taap.2013.07.014.

References

Abdollahi, A., Folkman, J., 2010. Evading tumor evasion: current concepts and perspectives of anti-angiogenic cancer therapy. Drug Resist. Updat. 13, 16–28.

Arafa el, S.A., Zhu, Q., Shah, Z.I., Wani, G., Barakat, B.M., Racoma, I., El-Mahdy, M.A., Wani, A.A., 2011. Thymoquinone up-regulates PTEN expression and induces apoptosis in doxorubicin-resistant human breast cancer cells. Mutat. Res. 706, 28–35.

Artacho-Cordon, F., Rios-Arrabal, S., Lara, P.C., Artacho-Cordon, A., Calvente, I., Nunez, M.I., 2012. Matrix metalloproteinases: potential therapy to prevent the development of second malignancies after breast radiotherapy. Surg. Oncol. 21, e143–e151.

Bai, L.Y., Omar, H.A., Chiu, C.F., Chi, Z.P., Hu, J.L., Weng, J.R., 2011. Antitumor effects of (S)-HDAC42, a phenylbutyrate-derived histone deacetylase inhibitor, in multiple myeloma cells. Cancer Chemother. Pharmacol. 68, 489–496.

Bergers, G., Hanahan, D., 2008. Modes of resistance to anti-angiogenic therapy. Nat. Rev. Cancer 8, 592–603.

Byrne, A.M., Bouchier-Hayes, D.J., Harmey, J.H., 2005. Angiogenic and cell survival functions of vascular endothelial growth factor (VEGF). J. Cell. Mol. Med. 9, 777–794.

Carmeliet, P., 2005. VEGF as a key mediator of angiogenesis in cancer. Oncology 69 (Suppl. 3), 4–10.

Chabut, D., Fischer, A.M., Colliec-Jouault, S., Laurendeau, I., Matou, S., Le Bonniec, B., Helley, D., 2003. Low molecular weight fucoidan and heparin enhance the basic fibroblast growth factor-induced tube formation of endothelial cells through heparan sulfate-dependent alpha6 overexpression. Mol. Pharmacol. 64, 696–702.

Cheung, A.K., Ko, J.M., Lung, H.L., Chan, K.W., Stanbridge, E.J., Zabarovsky, E., Tokino, T., Kashima, L., Suzuki, T., Kwong, D.L., Chua, D., Tsao, S.W., Lung, M.L., 2011. Cysteine-rich intestinal protein 2 (CRIP2) acts as a repressor of NF-kappaB-mediated proangiogenic cytokine transcription to suppress tumorigenesis and angiogenesis. Proc. Natl. Acad. Sci. U. S. A. 108, 8390–8395.

Coussens, L.M., Fingleton, B., Matrisian, L.M., 2002. Matrix metalloproteinase inhibitors and cancer: trials and tribulations. Science 295, 2387–2392.

Dell'Eva, R., Ambrosini, C., Vannini, N., Piaggio, G., Albini, A., Ferrari, N., 2007. AKT/NF-kappaB inhibitor xanthohumol targets cell growth and angiogenesis in hematologic malignancies. Cancer 110, 2007–2011.

Folkman, J., 1995. Angiogenesis in cancer, vascular, rheumatoid and other disease. Nat. Med. 1, 27–31.

Hung, W.C., Chang, H.C., 2009. Indole-3-carbinol inhibits Sp1-induced matrix metalloproteinase-2 expression to attenuate migration and invasion of breast cancer cells. J. Agric. Food Chem. 57, 76–82.

Hurwitz, H., Fehrenbacher, L., Novotny, W., Cartwright, T., Hainsworth, J., Heim, W., Berlin, J., Baron, A., Griffing, S., Holmgren, E., Ferrara, N., Fyfe, G., Rogers, B., Ross, R., Kabbinavar, F., 2004. Bevacizumab plus irinotecan, fluorouracil, and leucovorin for metastatic colorectal cancer. N. Engl. J. Med. 350, 2335–2342.

Khurana, R., Simons, M., Martin, J.F., Zachary, I.C., 2005. Role of angiogenesis in cardiovascular disease: a critical appraisal. Circulation 112, 1813–1824.

Kitamura, T., Asai, N., Enomoto, A., Maeda, K., Kato, T., Ishida, M., Jiang, P., Watanabe, T., Usukura, J., Kondo, T., Costantini, F., Murohara, T., Takahashi, M., 2008. Regulation of VEGF-mediated angiogenesis by the Akt/PKB substrate Girdin. Nat. Cell Biol. 10, 329–337.

Klein, G., Vellenga, E., Fraaije, M.W., Kamps, W.A., de Bont, E.S., 2004. The possible role of matrix metalloproteinase (MMP)-2 and MMP-9 in cancer, e.g. acute leukemia. Crit. Rev. Oncol. Hematol. 50, 87–100.

Kulp, S.K., Chen, C.S., Wang, D.S., Chen, C.Y., 2006. Antitumor effects of a novel phenylbutyrate-based histone deacetylase inhibitor, (S)-HDAC-42, in prostate cancer. Clin. Cancer Res. 12, 5199–5206.

Liekens, S., Bronckaers, A., Hernandez, A.I., Priego, E.M., Casanova, E., Camarasa, M.J., Perez-Perez, M.J., Balzarini, J., 2006. 5′-O-tritylated nucleoside derivatives: inhibition of thymidine phosphorylase and angiogenesis. Mol. Pharmacol. 70, 501–509.

Morais, C., Gobe, G., Johnson, D.W., Healy, H., 2009. Anti-angiogenic actions of pyrrolidine dithiocarbamate, a nuclear factor kappa B inhibitor. Angiogenesis 12, 365–379.

Nacev, B.A., Liu, J.O., 2011. Synergistic inhibition of endothelial cell proliferation, tube formation, and sprouting by cyclosporin A and itraconazole. PLoS One 6, e24793–e24802.

Omar, H.A., Sargeant, A.M., Weng, J.R., Wang, D., Kulp, S.K., Chen, C.S., 2009. Targeting of the Akt-nuclear factor-kappa B signaling network by [1-(4-chloro-3-nitrobenzenesulfonyl)-1H-indol-3-yl]-methanol (OSU-A9), a novel indole-3-carbinol derivative, in a mouse model of hepatocellular carcinoma. Mol. Pharmacol. 76, 957–968.

Omar, H.A., Berman-Booty, L., Weng, J.R., 2012. Energy restriction: stepping stones towards cancer therapy. Future Oncol. 8, 1503–1506.

Reddy, A.S., Zhang, S., 2013. Polypharmacology: drug discovery for the future. Expert. Rev. Clin. Pharmacol. 6, 41–47.

Roomi, M.W., Monterrey, J.C., Kalinovsky, T., Rath, M., Niedzwiecki, A., 2010. In vitro modulation of MMP-2 and MMP-9 in human cervical and ovarian cancer cell lines by cytokines, inducers and inhibitors. Oncol. Rep. 23, 605–614.

Roy, R., Yang, J., Moses, M.A., 2009. Matrix metalloproteinases as novel biomarkers and potential therapeutic targets in human cancer. J. Clin. Oncol. 27, 5287–5297.

Schram, K., De Girolamo, S., Madani, S., Munoz, D., Thong, F., Sweeney, G., 2010. Leptin regulates MMP-2, TIMP-1 and collagen synthesis via p38 MAPK in HL-1 murine cardiomyocytes. Cell. Mol. Biol. Lett. 15, 551–563.

Shiojima, I., Walsh, K., 2002. Role of Akt signaling in vascular homeostasis and angiogenesis. Circ. Res. 90, 1243–1250.

Singh, R.P., Dhanalakshmi, S., Agarwal, C., Agarwal, R., 2005. Silibinin strongly inhibits growth and survival of human endothelial cells via cell cycle arrest and downregulation of survivin, Akt and NF-kappaB: implications for angioprevention and antiangiogenic therapy. Oncogene 24, 1188–1202.

Szinwong, M., Sidek, S.M., Mahmud, R., Stanslas, J., 2013. Molecular targets in the discovery and development of novel antimetastatic agents: current progress and future prospects. Clin. Exp. Pharmacol. Physiol. 40, 307–319.

Tammali, R., Reddy, A.B., Srivastava, S.K., Ramana, K.V., 2011. Inhibition of aldose reductase prevents angiogenesis in vitro and in vivo. Angiogenesis 14, 209–221.

Tang, J.Y., Li, S., Li, Z.H., Zhang, Z.J., Hu, G., Cheang, L.C., Alex, D., Hoi, M.P., Kwan, Y.W., Chan, S.W., Leung, G.P., Lee, S.M., 2010. Calycosin promotes angiogenesis involving estrogen receptor and mitogen-activated protein kinase (MAPK) signaling pathway in zebrafish and HUVEC. PLoS One 5, e11822–e11835.

Tate, C.M., Blosser, W., Wyss, L., Evans, G., Xue, Q., Pan, Y., Stancato, L., 2013. LY2228820 dimesylate, a selective inhibitor of p38 mitogen-activated protein kinase, reduces angiogenic endothelial cord formation in vitro and in vivo. J. Biol. Chem. 288, 6743–6753.

Waas, E.T., Lomme, R.M., DeGroot, J., Wobbes, T., Hendriks, T., 2002. Tissue levels of active matrix metalloproteinase-2 and -9 in colorectal cancer. Br. J. Cancer 86, 1876–1883.

Wang, M., Wang, T., Liu, S., Yoshida, D., Teramoto, A., 2003. The expression of matrix metalloproteinase-2 and -9 in human gliomas of different pathological grades. Brain Tumor Pathol. 20, 65–72.

Wang, X.Y., Ju, S., Li, C., Peng, X.G., Chen, A.F., Mao, H., Teng, G.J., 2012. Non-invasive imaging of endothelial progenitor cells in tumor neovascularization using a novel dual-modality paramagnetic/near-infrared fluorescence probe. PLoS One 7, e50575–e50586.

Weng, J.R., Tsai, C.H., Kulp, S.K., Wang, D., Lin, C.H., Yang, H.C., Ma, Y., Sargeant, A., Chiu, C.F., Tsai, M.H., Chen, C.S., 2007. A potent indole-3-carbinol derived antitumor agent with pleiotropic effects on multiple signaling pathways in prostate cancer cells. Cancer Res. 7, 7815–7824.

Weng, J.R., Tsai, C.H., Omar, H.A., Sargeant, A.M., Wang, D., Kulp, S.K., Shapiro, C.L., Chen, C.S., 2009. OSU-A9, a potent indole-3-carbinol derivative, suppresses breast tumor growth by targeting the Akt-NF-kappaB pathway and stress response signaling. Carcinogenesis 30, 1702–1709.

Weng, J.R., Bai, L.Y., Omar, H.A., Sargeant, A.M., Yeh, C.T., Chen, Y.Y., Tsai, M.H., Chiu, C.F., 2010. A novel indole-3-carbinol derivative inhibits the growth of human oral squamous cell carcinoma in vitro. Oral Oncol. 46, 748–754.

Wilhelm, S.M., Adnane, L., Newell, P., Villanueva, A., Llovet, J.M., Lynch, M., 2008. Preclinical overview of sorafenib, a multikinase inhibitor that targets both Raf and VEGF and PDGF receptor tyrosine kinase signaling. Mol. Cancer Ther. 7, 3129–3140.

Wu, L.W., Mayo, L.D., Dunbar, J.D., Kessler, K.M., Baerwald, M.R., Jaffe, E.A., Wang, D., Warren, R.S., Donner, D.B., 2000. Utilization of distinct signaling pathways by receptors for vascular endothelial cell growth factor and other mitogens in the induction of endothelial cell proliferation. J. Biol. Chem. 275, 5096–5103.

Wu, G., Luo, J., Rana, J.S., Laham, R., Sellke, F.W., Li, J., 2006. Involvement of COX-2 in VEGF-induced angiogenesis via P38 and JNK pathways in vascular endothelial cells. Cardiovasc. Res. 69, 512–519.

Yue, P., Gao, Z.H., Xue, X., Cui, S.X., Zhao, C.R., Yuan, Y., Yin, Z., Inagaki, Y., Kokudo, N., Tang, W., Qu, X.J., 2011. Des-gamma-carboxyl prothrombin induces matrix metalloproteinase activity in hepatocellular carcinoma cells by involving the ERK1/2 MAPK signalling pathway. Eur. J. Cancer 47, 1115–1124.